2012

Dendrimer-fullerenol soft-condensed nanoassembly

Priyanka Bhattacharya
Clemson University

Seung Ha Kim
Iowa State University, shkim@iastate.edu

Pengyu Chen
Clemson University

See next page for additional authors

THE JOURNAL OF PHYSICAL CHEMISTRY C

Article

pubs.acs.org/JPCC

Dendrimer–Fullerenol Soft-Condensed Nanoassembly

Priyanka Bhattacharya,[†] Seung Ha Kim,[‡] Pengyu Chen,[†] Ran Chen,[†] Anne M. Spuches,[§] Jared M. Brown,[∥] Monica H. Lamm,[‡] and Pu Chun Ke*[,†]

[†]Department of Physics and Astronomy, COMSET, Clemson University, Clemson, South Carolina 29634, United States

[‡]Department of Chemical and Biological Engineering, Iowa State University, Ames, Iowa 50011, United States

[§]Department of Chemistry, East Carolina University, Greenville, North Carolina 27858, United States

[∥]Department of Pharmacology & Toxicology, East Carolina University, Greenville, North Carolina 27834, United States

Supporting Information

ABSTRACT: Nanoscale assembly is an area of research that has vast implications for molecular design, sensing, nanofabrication, supramolecular chemistry, catalysis, and environmental remediation. Here we show that poly(amidoamine) (PAMAM) dendrimers of both generations 1 (G1) and 4 (G4) can host 1 fullerenol per 2 dendrimer primary amines as evidenced by isothermal titration calorimetry, dynamic light scattering, and spectrofluorometry. Thermodynamically, the interactions were similarly spontaneous between both generations of dendrimers and fullerenols, however, G4 formed stronger complexes with fullerenols resulting from their higher surface charge density and more internal voids, as demonstrated by spectrofluorometry. In addition to hydrogen bonding that existed between the dendrimer primary amines and the fullerenol oxygens, hydrophobic and electrostatic interactions also contributed to complex formation and dynamics. Such a hybrid of soft and condensed nanoassembly may have implications for environmental remediation of discharged nanomaterials and entail new applications in drug delivery.

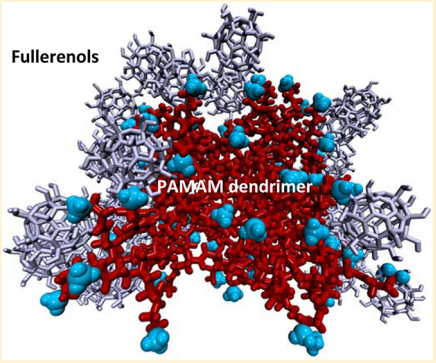

1. INTRODUCTION

Nanoscale assembly is an area of active research that has great implications for molecular design, biological sensing, environmental remediation, nanofabrication, supramolecular chemistry, energy, and catalysis.[1,2] Among the promising nanoscale scaffolds, dendrimers are a class of polymeric nanomaterials that possess high degree branching and order, low viscosity, monodispersity, pH-responsive surface charge and radius of gyration, and ample interior voids.[3,4] Major classes of dendritic polymers such as poly(amidoamine) (PAMAM), poly(propylene imine) (PPI), and PAMAM-tris(hydroxymethyl) amidomethane have been shown robust in encapsulating guest species of metal cations and anions, polycyclic aromatic hydrocarbons, and inorganic solutes in contaminated waters and soils.[5−10] Specifically, within the pH range of 7−10 PAMAM dendrimers bind to transition metals through multiple mechanisms, including Lewis acid−base complexation with their primary and tertiary amines serving as donors, ion-pairing with charged terminal groups, and nonspecific interactions that result from the physical encapsulation of ions in interior cavities which may involve interactions with trapped counterions or water molecules.[6,7,10−12] Generally, lower-generation dendrimers bind to guest molecules or ions more effectively due to their more accessible interior which offers decreased mass transfer resistance and facilitates more guest−host collisions than their higher generation counterparts.[11] Importantly, dendrimers can also reversibly release contaminant loads through changes in the solvent pH and electrolyte strength, or via a UV trigger. For example, using PAMAM and PPI dendrimers Diallo et al.[6,7] selectively removed Cu(II) and perchlorate (ClO_4^-) from water. Once dendrimer−Cu(II) or dendrimer−ClO_4^- complexes were formed, they were eliminated from aqueous solutions by ultrafiltration. Regeneration of the dendrimers, at 90% or above, was realized when the solution pH was lowered to 4 to release Cu(II) and raised to 9 to unload ClO_4^-. The primary mechanism behind the regeneration lies in the pK_a values of the PAMAM primary (∼7) and tertiary (∼4) amines.[13] Specifically, protonation of the dendrimer tertiary amines coordinating with the Cu(II) at pH 4 resulted in electrostatic repulsion, whereas deprotonation of the dendrimer primary amines at pH 9 reduced their attractions for ClO_4^-. Within the scope of dendrimer host−guest assembly,[14] molecular dynamics simulations have shown that protonation of the dendrimer amines favors intermolecular hydrogen bonding with guest species, in addition to other noncovalent intermolecular forces such as ionic bonding and polar and van der Waals forces.[15] Furthermore, dendrimers can be integrated into existing, commercial ultrafiltration membrane separation processes that permit operation at lower pressure (and thus lower cost) than that normally applied to reverse osmosis membranes for water purification.[6]

Received: April 16, 2012
Revised: June 14, 2012
Published: July 3, 2012

In addition to environmental and industrial applications, dendrimers can bind either covalently or noncovalently with small and macro-biomolecules as well as metal ions, and act as transporters for the delivery of genes, drugs, prodrugs, MRI contrast agents, and viral inhibitors.[4,16,17] The feasibility of such applications is established upon the understanding that PAMAM dendrimers interact readily with phospholipids and show high permeability through cell membranes,[18−20] thereby rendering them nonviral transporters with high efficacy.[21] The biocompatibility of dendrimers has been a topic of concern, but toxicities were reported for PAMAM dendrimers of generations seven and larger, and only minimally.[22,23] Additionally, the toxicity of PAMAM dendrimers can be mitigated by neutralizing or converting their surface charge to anionic.[24]

In contrast to the "soft" polymeric dendrimers, fullerenes and their derivatives are carbon-based, single-molecular particulates that possess appealing mechanical, thermal, electrical, physicochemical, and redox properties; the last two aspects endowed them with the name "nanopharmaceuticals".[25−28] Consequently, fullerenes and their derivatives are building blocks for designing nanoscaled assemblies for promising physical, biological, and medicinal applications. For example, photovoltaic devices made of polymer-fullerene derivatives—where the polymer acts as the electron donor and the fullerene as the electron acceptor—have been studied and commercialized.[29] Conjugation of murine anti-gp240 melanoma antibody to fullerene C_{60} with cross-linker *N*-succinimidyl-3-(2-pyridyldithio)propionate (SPDP) has been shown to preserve the drug potency and facilitate the development of fullerene immunotherapy.[30]

Hydrophobic fullerenes C_{60} and C_{70} show a propensity for the amphiphilic lipid bilayer and can potentially impact cellular processes including electron transport in the photosystems of plant species. Water-soluble fullerene derivatives $C_{60}(OH)_x$—or fullerenols—have been found effective in suppressing reactive oxygen species and the toxicity of copper, and have been employed as glutamate receptor antagonists and antiproliferative, neuroprotective, or anticancer agents.[28,31−33] Along with these biological and medicinal applications, the fate of fullerenes and their derivatives in living systems has become a topic of much research effort, especially over the past decade.[34−39] Using *in vitro* and *in silico* studies Sayes et al.[36] and Qiao et al.[37] delineated the differential cytotoxicities of pristine and functionalized fullerenes, and attributed such contrasting cell responses to lipid peroxidation, hydrophobicity, and distribution of potential of mean force associated with the nanoparticles in a lipid bilayer. Others[40] and our group[41,42] showed that fullerenol could inhibit polymerase chain reaction (PCR) and microtubule polymerization *in vitro*. Specifically, the surface hydroxyls of fullerenol $C_{60}(OH)_{20}$ complexed with the triphosphate oxygens of nucleotides and nucleic acids and with the alpha helices and the junctions of tubulin dimers through hydrogen bonding (H-bonding), as well as hydrophobic and electrostatic interactions. In addition, water-soluble $C_{60}(OH)_{20}$ compromised plasma membranes to induce necrosis in *Allium cepa* cells, driven by concentration gradient of the nanoparticles across the hydrophobic plant cell wall.[43]

In view of the promises of fullerenes and dendrimers for nanomedicine, and in view of the crucial need for developing new strategies for mitigating the potential adverse effects of environmental discharge of nanomaterials, here we show a novel self-assembly of PAMAM dendrimers and fullerenols and elucidate the underlying physical chemistry and thermodynamics for such assembly. Both generations 1 and 4 (i.e., G1 and G4) dendrimers have been employed to take advantage of their versatile morphology, charge density (8 and 64 primary amines per G1 and G4 dendrimer, respectively), and radius of gyration. In addition to providing a fundamental basis for dendrimer environmental applications and drug delivery, this study also serves as a proof-of-concept that nanomaterial discharge—an emerging environmental concern—may be remedied by alternative nanotechnologies.

2. EXPERIMENTAL SECTION

2.1. Materials. Amine terminated PAMAM dendrimers with ethylenediamine cores of generations 1 (MW 1430, 9.98 wt % in H_2O) and 4 (MW 14,215, 14.04 wt % in H_2O) (G1 and G4, respectively) were purchased as aqueous solutions from Dendritech, Inc. Polyhydroxy-C60 ($C_{60}(OH)_n$, fullerenol hereafter, $n \sim 18-22$) was purchased from BuckyUSA. An average of 20 OH groups per fullerenol molecule was assumed for all measurements. All materials were used as received. The stock fullerenol suspension of 1 mM was prepared in deionized water by bath sonication for 30 min.

2.2. Dynamic Light Scattering and Zeta Potential Measurements. The average hydrodynamic diameter, particle size distribution, and polydispersity indices (PDI) of the dendrimer−fullerenol assemblies were measured using a Nanosizer (S90, Malvern Instruments). The pristine dendrimer and fullerenol aqueous solutions were filtered with Anotop filters (Whatman) of 20 nm pore size prior to the measurements. Nineteen injections of dendrimer solutions of 8 μL each were added to 1.46 mL of fullerenol suspension in a standard plastic macrocuvette of path length 1 cm. The dendrimer−fullerenol mixtures were allowed to incubate for 5 min after each successive injection and 30 s mixing prior to the measurements. The pH of the final mixture was 6.5. Three repeats were performed for statistical error analysis. Surface charges of the pristine dendrimer and fullerenol suspensions and that of the dendrimer−fullerenol mixtures at different stoichiometric ratios were measured using a Zetasizer (NanoZS, Malvern Instruments).

2.3. Isothermal Titration Calorimetry (ITC). ITC was performed with a VP-ITC isothermal titration microcalorimeter (MicroCal, Inc.) with dendrimers in the injection syringe and fullerenol in the experimental cell, while the reference cell contained deionized water. Concentration of fullerenol in the experimental cell was 10 μM (0.0106 g/L) for reactions with G1 dendrimer and 100 μM (0.106 g/L) for G4 dendrimer. The concentrations of G1 and G4 dendrimers in the injection syringe were 200 μM and 50 μM, respectively. The initial volume of fullerenol in the reaction cell was 1.46 mL. Each experimental run consisted of 31 to 35 injections of 8 μL each at an interval of 3 min between successive injections. The sample cell was maintained at 25 °C and stirred at 200 rpm. Heats of dilution of dendrimers were subtracted from the final ITC results. Due to the negligible dilution of fullerenol, heats of dilution of fullerenol were minimal. Apparatus cleaning was performed according to the manufacturer's recommendations prior to the experiments. Baseline corrections and data fitting were performed using automated routines in Origin v.7.0 data analysis and acquisition software (OriginLab Corp.). Minor corrections were done at the user's discretion. Figure 2 shows the raw ITC data of power vs time, and the resulting peak integrations are plotted as energy per mole of injectant (ΔH) vs the molar ratio of dendrimers per fullerenol (n) in the sample

cell after each injection. Analysis of the ITC data was done using the *One set of sites* model. Due to the larger size of dendrimers compared to fullerenols, in our experiments, dendrimers were considered as macromolecules and fullerenols as ligands. Hence, during data analysis, a selection of "Ligand in Cell" was made. A much larger raw heat is observed in the case of G4 dendrimers than in the case of G1 dendrimers since, in the case of G4 dendrimers, 44 fullerenols bind to each dendrimer instantaneously releasing a larger amount of heat, whereas only one fullerenol binds to G1. It is noted that, with fullerenols in the injection syringe and dendrimers in the experimental cell, we would have observed a lesser raw heat release due to the presence of excess dendrimers and fewer fullerenols. In such a case, it would have taken a longer time to reach saturation in heat release.

2.4. Fluorescence Spectroscopy. A Cary Eclipse fluorescence spectrophotometer (Varian, Inc.) was used to measure the fluorescence of the dendrimer−fullerenol assemblies. 1 μL of aqueous dendrimer solution was added in gradient concentrations to 500 μL of fullerenol in a 1 mm path length quartz cuvette and allowed to incubate for 5 min after a 30 s mixing. Spectrum scans between 400 and 600 nm of the fluorescence emitted by the control samples and the mixture upon excitation at 340 nm were conducted after 5 min incubation each time. Fluorescence intensities were recorded until complete quenching was observed. Measurements were repeated with three samples for statistical error analysis. Recorded fluorescence spectra were corrected for their respective blanks (i.e., fullerenols and dendrimers only).

3. RESULTS AND DISCUSSION

3.1. An Empirically Determined Ratio of Dendrimer−Fullerenol Assembly. As shown in Table 1, the hydrodynamic diameter of fullerenol averaged 4.4 ± 3.8 nm at 10 μM and 5.1 ± 5.1 nm at 100 μM, indicating partial association of fullerenols as a result of hydrophobic and hydrophilic partitioning. The zeta potentials of both G1 and G4 dendrimers were positive due to their protonated primary amines at neutral pH (Table 1). Upon addition of G1 and G4 dendrimers to fullerenol solutions, however, the average hydrodynamic diameter of the dendrimer−fullerenol assembly increased immediately by an order of magnitude (Figure 1). Also, the stoichiometric ratio of greater than one fullerenol per primary amine suggested that their binding was more complex than ionic bonding, likely also involving hydrogen bonding (H-bonding) and hydrophobic interaction. For G1 dendrimer, saturation in the aggregate size was observed ranging between 710 and 955 nm, for a G1/fullerenol molar ratio of 0.27 (corresponding to 2.19 primary amines per fullerenol) or higher (Figure 1A). For G4 dendrimer, uniform sized aggregates were formed until the ratio of dendrimer/fullerenol reached ~0.03 (corresponding to 2.14 primary amines/fullerenol, see Figure 1B). As more dendrimers were added to the suspensions, the fullerenols associated with one dendrimer started to interact with those bound to neighboring dendrimers to trigger the formation of dendrimer−fullerenol supramolecular complexes, likely mediated by H-bonding. Such intercluster interactions also occurred in the case of the G1/fullerenol system. Interestingly, the number of primary amines/fullerenol at which intercluster aggregation occurred was ~2 for both G1 and G4 dendrimers. Whereas the sizes of the G1/fullerenol and G4/fullerenol complexes were comparable

Table 1. Characterizations of Fullerenols, PAMAM Dendrimers, and Their Assemblies

particle	hydrodynamic size (nm)	polydispersity index (PDI)	zeta potential (mV)
$C_{60}OH_{20}$ (10 μM)	4.4 ± 3.8	1.00 ± 0.00	−21.8 ± 10.9
$C_{60}OH_{20}$ (100 μM)	5.1 ± 5.1	0.68 ± 0.22	−53.8 ± 10.5
G1-NH_2 (200 μM)	2.5 ± 1.6	0.84 ± 0.12	24.7 ± 3.0
G4-NH_2 (50 μM)	5.3 ± 1.3	0.74 ± 0.06	23.6 ± 4.8
[G1]/[$C_{60}OH_{20}$] = 0.05	79.18	0.25 ± 0.03	−25.0 ± 6.5
[G1]/[$C_{60}OH_{20}$] = 1.37	1071	0.24 ± 0.04	9.7 ± 6.4
[G4]/[$C_{60}OH_{20}$] = 0.001	196.7	0.18 ± 0.02	−52.1 ± 4.9
[G4]/[$C_{60}OH_{20}$] = 0.04	403.2	0.20 ± 0.03	−12.7 ± 7.8

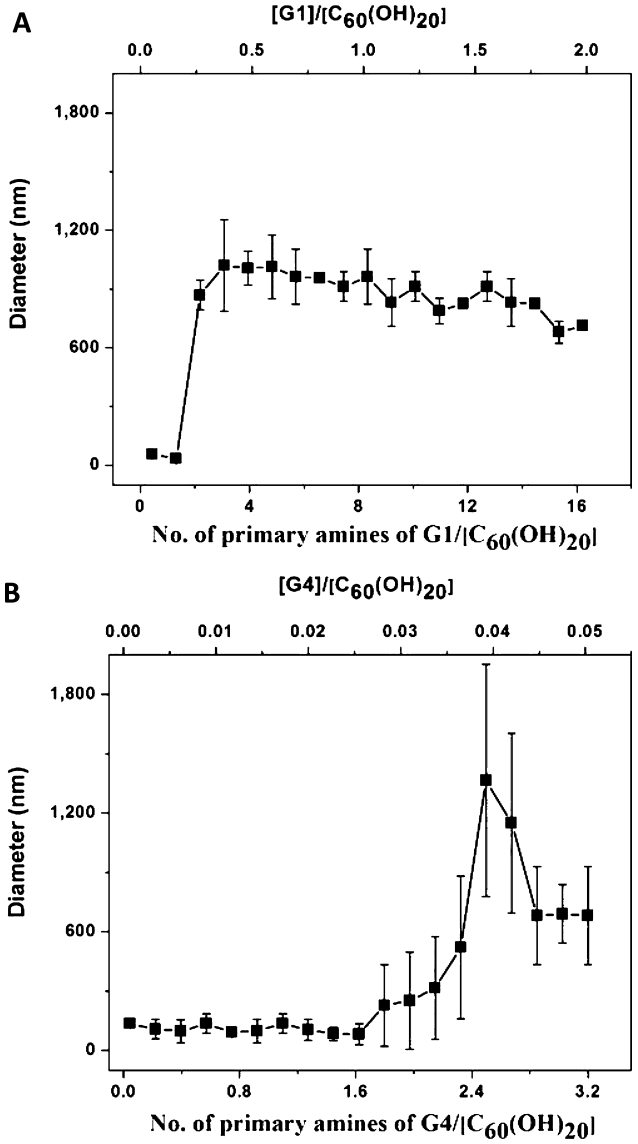

Figure 1. DLS measurements of (A) G1/fullerenol and (B) G4/fullerenol complexes. An abrupt increase in the hydrodynamic size of the complexes was observed for both G1/fullerenol and G4/fullerenol mixtures at a ratio of number of primary amines of dendrimer/fullerenol ≈2.

dx.doi.org/10.1021/jp3036692 | J. Phys. Chem. C 2012, 116, 15775−15781

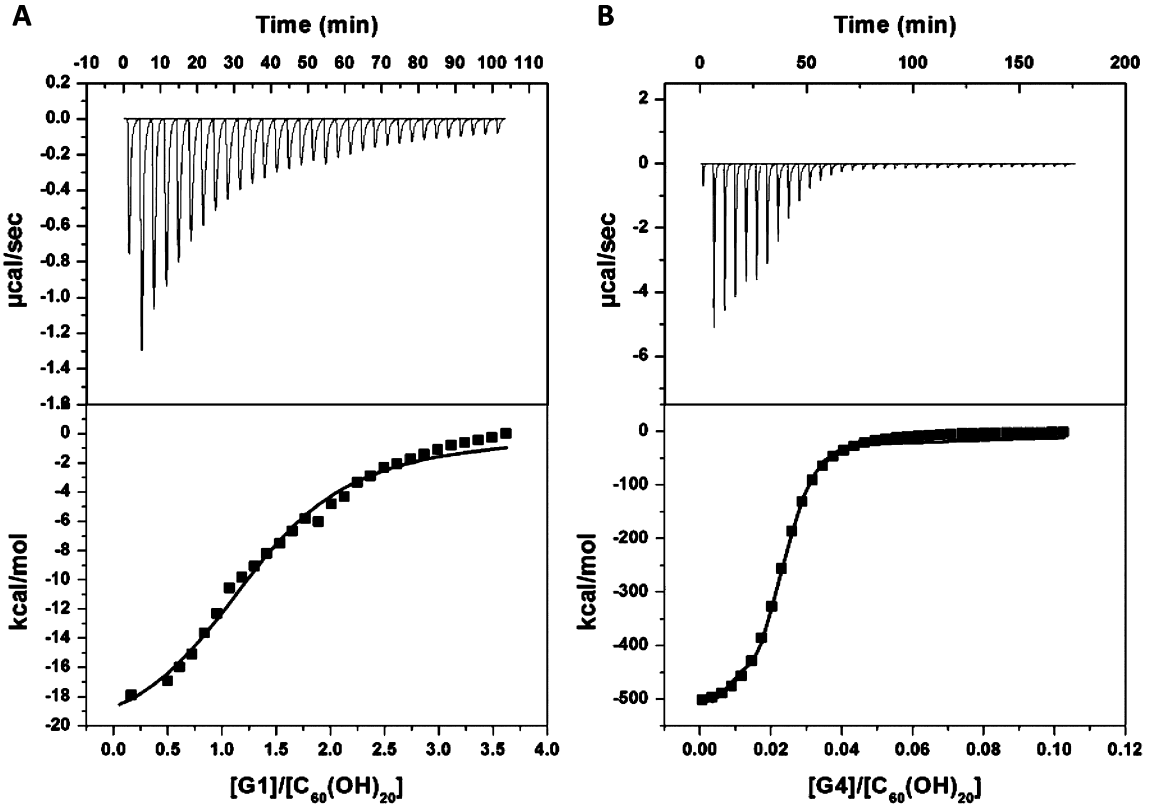

Figure 2. ITC raw data and analysis plots of (A) G1/fullerenol and (B) G4/fullerenol complexes. The interactions between dendrimers and fullerenols resulted in significant heat release (ΔH = −21.8 kcal/mol for G1/fullerenol and −19.5 kcal/mol for G4/fullerenols). The fullerenol:dendrimer stoichiometric ratios obtained from data analysis were 1.34 ± 0.04 for G1/fullerenol and 44.1 ± 0.43 for G4/fullerenol. The ΔG values for both G1/fullerenol (−7.69 kcal/mol) and G4/fullerenol (−7.24 kcal/mol) indicate the reactions are similarly spontaneous. G1/fullerenol complexes are also more ordered ($\Delta S = -47.4 \times 10^{-3}$ kcal/mol) than G4/fullerenol complexes ($\Delta S = -15.8 \times 10^{-3}$ kcal/mol).

(1,000−1,300 nm) at a primary amine/fullerenol ratio of ∼2, precipitation occurred more rapidly for G4 dendrimers (See Figure 1 and Figure S1 of the Supporting Information), implying a stronger G4/fullerenol association.

3.2. Thermodynamics of Dendrimer−Fullerenol Assembly. The enthalpic change (ΔH) of dendrimer−fullerenol binding indicated a net exothermic reaction (Figure 2). As fullerenols in suspension were being consumed by dendrimers, the heat released upon each dendrimer−fullerenol binding decreased to reach a near saturation. The reactions were spontaneous, as indicated by the negative Gibbs free energy ΔG. Upon binding to fullerenols the much lower entropy ΔS of G1 dendrimers in contrast to that of G4 dendrimers implies a higher degree of ordering in the G1/fullerenol system. This higher entropic change for G1 dendrimers is understandable considering they are more flexible or less organized than G4 dendrimers in free solution and could become "frozen" upon complexation with fullerenols. The binding constants derived from the ITC measurement were 4.35×10^5 M^{-1} and 2.69×10^5 M^{-1} for the G1/fullerenol and G4/fullerenol systems. For G1 dendrimer, whose size is comparable to that of fullerenol, the binding stoichiometric ratio n of fullerenol to dendrimer was ∼1. Consistent with the DLS data, which showed formation of dendrimer−fullerenol supramolecular complexes of nearly uniform sizes above a G1/fullerenol molar ratio of 0.27 (corresponding to 2.19 primary amines of G1/fullerenol), a gradually decreasing heat release above this ratio was observed; this suggests lingering interactions between the dendrimer−fullerenol aggregates. For G4 dendrimer, by contrast, the binding stoichiometric ratio was nearly proportional to the number of primary amines (64) on the dendrimer, at 44.1. The binding curves also suggest that saturation was reached faster in the case of G4 dendrimer at a G4/fullerenol ratio of 0.04 (corresponding to 2.14 primary amines of G1/fullerenol), implying completion of the binding and in agreement with the DLS data (Figure 1). Such saturation was not reached for G1 dendrimers, perhaps due to the presence of free fullerenols.

Whereas the spontaneity of the interactions between G1 and G4 dendrimers with fullerenols was similar, the entropy and enthalpy of the G4 dendrimer−fullerenol interaction were slightly less than those between G1 dendrimer and fullerenols. This could be attributed to the more open and hydrophilic structure of G1 over G4 dendrimers. At neutral pH, both the interiors of G1 and G4 PAMAM dendrimers remained hydrophobic, while their exterior primary amines were protonated. Fullerenols, however, were partially negatively charged at neutral pH, resulting from the high electronegativity of the surface oxygens and deprotonation of the surface hydroxyl groups ($pK_a \sim 4$).[44] The assembly of dendrimer−fullerenol was therefore possibly mediated by ionic interactions between the protonated dendrimer amines and the negatively charged fullerenol oxygens, as well as by H-bonding between the fullerenol surface oxygens and the hydrogens on the dendrimer amine groups.

3.3. Intermolecular Interactions in Dendrimer−Fullerenol Assembly. As shown in Figure 3, increased dendrimer concentrations resulted in the quenching of fullerenol

dx.doi.org/10.1021/jp3036692 | J. Phys. Chem. C 2012, 116, 15775−15781

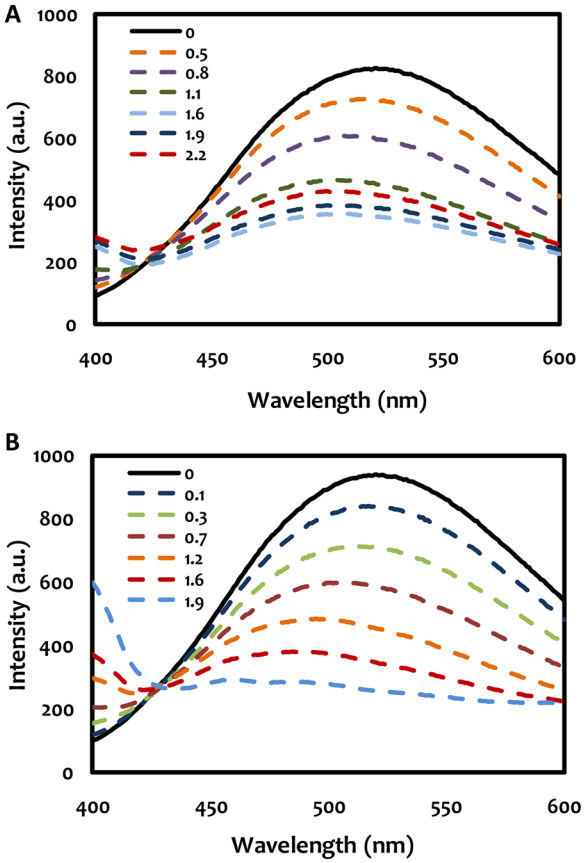

Figure 3. Fluorescence emission of fullerenol in the presence of increasing amounts of (A) number of primary amines of G1 per fullerenol = 0, 0.5, 0.8, 1.1, 1.6, 1.9, and 2.2; and (B) number of primary amines of G4 per fullerenol = 0, 0.1, 0.3, 0.7, 1.2, 1.6, and 1.9.

fluorescence,[45,46] which was accompanied by a shift in the fluorescence maximum. This indicates that, upon excitation, dendrimers and fullerenols formed charge-transfer complexes. In the case of G1 dendrimer, above a ratio of 1.9 for the number of primary amines/fullerenol, scattering from large aggregates resulted in a slight increase in fluorescence, whereas precipitation of the large aggregates above that ratio in the case of G4/fullerenol prevented further measurements. The fluorescence intensity of fullerenols alone was linearly dependent on its concentration (see Figure S2 of the Supporting Information). Dendrimers, in comparison, displayed weak concentration dependence for their autofluorescence (see Figure S3 of the Supporting Information). However, quenching and peak shift upon fullerenol binding with dendrimers were notable. Specifically, a blue shift of 21 nm, averages for both G1- and G4-fullerenol, was observed for increased concentrations of dendrimers bound with fullerenols. Charge-transfer complexes could be formed between the hydroxyl groups of fullerenol and the protons on the amines of dendrimers. Quenching of fluorescence can be described by the Stern–Volmer equation as[47]

$$\frac{F_0}{F} = (1 + K_{SV}[Q])(\exp[Q]) \quad (1)$$

where F_0 and F are the fluorescence intensities of the fluorophore (fullerenol) in the absence and presence of a quencher (dendrimer), respectively, K_{SV} and V are the Stern–Volmer and sphere-of-action quenching constants, and [Q] is the concentration of the quencher (dendrimer). As seen in Figure 4, the Stern–Volmer plot is nonlinear with a positive

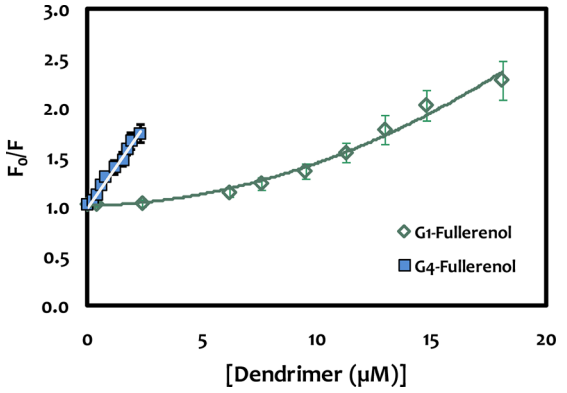

Figure 4. Stern–Volmer plots for G1/fullerenol and G4/fullerenol complexes. G1/fullerenol complexes show coexistence of static and dynamic quenching with a positive deviation in the plot, whereas G4/fullerenol complexes show primarily dynamic quenching, indicated by the linearity of the plot.

deviation for G1/fullerenol complexes, indicating simultaneous occurrence of both dynamic and static quenching. For low dendrimer concentrations, sphere-of-action quenching dominated. The value of V calculated from the data fitted with eq 1 yielded 0.028×10^5 M^{-1}. For higher dendrimer concentrations, dynamic or collisional quenching through charge-transfer, H-bonding, and electrostatic interactions between the already formed complexes and newly added dendrimers dominated, yielding $K_{SV} = 0.96 \times 10^5$ M^{-1}. A smaller value of V indicates that the fullerenol fluorescence was quenched primarily by dynamic quenching between the two species. In the case of G4/fullerenol, the Stern–Volmer plots are linear throughout (Figure 4), indicating the quenching was primarily dynamic. The linear Stern–Volmer constant K_{SV} obtained from the fitted data is 3.3×10^5 M^{-1}. The 3-fold higher value of K_{SV} for G4/fullerenol complexes is due to the larger surface area of the G4 dendrimers which offers many more intermolecular contacts with fullerenol aggregates than those observed for G1 dendrimers, thus increasing their efficiency for quenching fullerenols.

A modified Stern–Volmer equation (see eq 1 of the Supporting Information) offers new insight into the binding affinity of the static quenching process.[48] The value of binding constant obtained in the case of G4/fullerenol (2.64×10^5 M^{-1}) is in excellent agreement with our ITC results (2.69×10^5 M^{-1}). In contrast, the value in the case of G1/fullerenol (1.0×10^5 M^{-1}) is much lower than our ITC measurement (4.35×10^5 M^{-1}). Note that ITC measures the binding constant as a result of combined electrostatic interactions, complex formations, H-bonding, and hydrophobic interactions, whereas those obtained from fluorescence measurements primarily resulted from complex formation via ionic bonding and Lewis acid–base reaction. This reiterates our hypothesis that G4 formed stronger complexes with fullerenols than G1 throughout the concentration range used. However, complex formation between G1 and fullerenols was the strongest in the lower concentration region, after which large agglomerates were formed (as shown from the DLS data) due to other interactions through hydrogen bonding and hydrophobic interactions. The fraction of accessible fullerenols calculated from the modified

dx.doi.org/10.1021/jp3036692 | J. Phys. Chem. C 2012, 116, 15775–15781

Stern–Volmer equation (f_a = 1.09 for G1/fullerenol and 1.23 for G4/fullerenol) implies that, initially, there might be more than one binding site of fullerenol for dendrimers and the molecular environment of fullerenol was easily accessible to the dendrimer. In addition, the spectral shift observed could be attributed to selective quenching of exposed vs buried fluorophore sites of the fullerenol.[47]

4. CONCLUSIONS

The thermodynamics, stoichiometric ratio, and binding mechanisms of dendrimer–fullerenol assembly have been studied by the experimental techniques of DLS, ITC, and spectrophotometry. The formation of dendrimer–fullerenol assemblies, at a maximum loading capacity of ~2 or 44 fullerenols per G1 or G4 dendrimer (corresponding to ~2 primary amines per fullerenol in both cases), was found to be energetically favorable. In addition, intercluster interactions were evident, as a result of electrostatic forces, H-bonding, ionic bonding, and Lewis acid–base reaction. Apparently, such intercluster formation can be controlled by adjusting the concentrations of both the fullerenol and the dendrimer and by tuning the molar ratio of dendrimer to fullerenol. While intercluster interaction should be minimized for the delivery of fullerene derivatives by a dendrimer, in light of their diffusion in the bloodstream and eventual cell uptake, intercluster interaction is deemed desirable for mitigating the accidental release of nanomaterials in the environment. Based on our study, we recommend a G1/fullerenol loading ratio of 0.2–1.6, and G4/fullerenol loading ratio of 0.005–0.02 for drug delivery (the range below precipitation), and a G1/fullerenol loading ratio of above 1.6, and a G4/fullerenol loading ratio of above 0.02 for environmental remediation. Furthermore, for both nanomedicinal and environmental applications, the assembly of dendrimer and fullerenol—as exemplified in the current study—may be extended to that of branched/hyperbranched polymers and nanoparticles of opposite charge.

■ ASSOCIATED CONTENT

Supporting Information

Additional digital photo of dendrimer–fullerenol dispersions, fluorescence data of fullerenol and dendrimer control solutions, and the modified Stern–Volmer equation. This material is available free of charge via the Internet at http://pubs.acs.org.

■ AUTHOR INFORMATION

Corresponding Author

*E-mail: pcke11@clemson.edu. Tel: 864-656-0558. Fax: 864-656-0805.

Notes

The authors declare no competing financial interest.

■ ACKNOWLEDGMENTS

This work was supported by an NSF CAREER Award CBET-0744040 and US EPA Grant RD835182 to P.C.K., NSF Grants OCI-0749156 and OCI-0941434 to M.H.L., and NIH Grant RO1 #ES019311 to J.M.B. P.B. acknowledges a Grant-in-Aid of Research from Sigma Xi. The authors thank Apparao Rao for discussions and an anonymous reviewer for insightful comments.

■ REFERENCES

(1) Lehn, J. M. *Proc. Natl. Acad. Sci. U.S.A.* **2002**, *99*, 4763–4768.
(2) Lin, B. F.; Marullo, R. S.; Robb, M. J.; Krogstad, D. V.; Antoni, P.; Hawker, C. J.; Campos, L. M.; Tirrell, M. V. *Nano Lett.* **2011**, *11*, 3946–3950.
(3) Frechet, M. J.; Tomalia, D. A. *Dendrimers and other Dendritic Polymers*; Wiley and Sons: New York, 2001.
(4) Helms, B.; Meijer, E. W. *Science* **2006**, *313*, 929–930.
(5) Diallo, M. S.; Balogh, L.; Shafagati, A.; Johnson, J. H.; Goddard, W. A., III; Tomalia, D. A. *Environ. Sci. Technol.* **1999**, *33*, 820–824.
(6) Diallo, M. S.; Christie, S.; Swaminathan, P.; Johnson, J. H., Jr.; Goddard, W. A., III. *Environ. Sci. Technol.* **2005**, *39*, 1366–1377.
(7) Diallo, M. S.; Falconer, K.; Johnson, J. H., Jr.; Goddard, W. A., III. *Environ. Sci. Technol.* **2007**, *41*, 6521–6527.
(8) Diallo, M. S.; Arasho, W.; Johnson, J. H., Jr.; Goddard, W. A., III. *Environ. Sci. Technol.* **2008**, *42*, 1572–1579.
(9) Arkas, M.; Tsiourvas, D.; Paleos, C. M. *Chem. Mater.* **2003**, *15*, 2844–2847.
(10) Chen, P.; Yang, Y.; Bhattacharya, P.; Wang, P.; Ke, P. C. J. *Phys. Chem. C* **2011**, *115*, 12789–12796.
(11) Xu, Y.; Zhao, D. *Environ. Sci. Technol.* **2005**, *39*, 2369–2375.
(12) Bhattacharya, P.; Chen, P.; Spano, M. N.; Zhu, L.; Ke, P. C. *J. Appl. Phys.* **2011**, *109*, 014911–1–6.
(13) Tomalia, D. A.; Naylor, A. M.; Goddard, W. A., III. *Angew. Chem., Int. Ed. Engl.* **1990**, *29*, 138–175.
(14) Narayanan, V. V.; Newkome, G. R. *Top. Curr. Chem.* **1998**, *197*, 19–77.
(15) Tanis, I.; Karatasos, K. *Phys. Chem. Chem. Phys.* **2009**, *11*, 10017–10028.
(16) Voulgarakis, N. K.; Rasmussen, K. O.; Welch, P. M. *J. Chem. Phys.* **2009**, *130*, 155101-1–5.
(17) Lee, C. C.; MacKay, J. A.; Frechet, J. M. J.; Szoka, F. C. *Nat. Biotechnol.* **2005**, *23*, 1517–1526.
(18) Kelly, C. V.; Liroff, M. G.; Triplett, L. D.; Leroueil, P. R.; Mullen, D. G.; Wallace, J. M.; Meschinchi, S.; Baker, J. R., Jr.; Orr, B. G.; Banaszak Holl, M. M. *ACS Nano* **2009**, *3*, 1886–1896.
(19) Smith, P. E. S.; Brender, J. R.; Ulrich, H.; Durr, N.; Xu, J. D.; Mullen, D. G.; Banaszak Holl, M. M.; Ramamoorthy, A. *J. Am. Chem. Soc.* **2010**, *132*, 8087–8097.
(20) Hong, S.; Rattan, R.; Majoros, I. J.; Mullen, D. G.; Peters, J. L.; Shi, X. Y.; Bielinska, A. U.; Blanco, L.; Orr, B. G.; Baker, J. R., Jr.; et al. *Bioconjugate Chem.* **2009**, *20*, 1503–1513.
(21) Kukowska-Latallo, J. F.; Bielinska, A. U.; Johnson, J.; Spindler, R.; Tomalia, D. A.; Baker, J. R., Jr. *Proc. Natl. Acad. Sci. U.S.A.* **1996**, *93*, 4897–4902.
(22) Naha, P. C.; Davoren, M.; Casey, A.; Byrne, H. J. *Environ. Sci. Technol.* **2009**, *43*, 6864–6869.
(23) Mortimer, M.; Kasemets, K.; Heinlaan, M.; Kurvet, I.; Kahru, A. *Toxicol. In Vitro* **2008**, *22*, 1412–1417.
(24) Jevprasesphant, R.; Penny, J.; Jalal, R.; Attwood, D.; McKeown, N. B.; D'Emanuele, A. *Int. J. Pharm.* **2003**, *252*, 263–266.
(25) Bosi, S.; Da Ros, T.; Spalluto, G.; Prato, M. *Eur. J. Med. Chem.* **2003**, *33*, 913–923.
(26) Bakry, R.; Vallant, R. M.; Najam-ul-Haq, M.; Rainer, M.; Szabo, Z.; Huck, C. W.; Bonn, G. K. *Int. J. Nanomed.* **2007**, *2*, 639–649.
(27) Tegos, G. P.; Demidova, T. N.; Lopez, D. A.; Lee, H.; Wharton, T.; Gali, H.; Hamblin, M. R. *Chem. Biol.* **2005**, *12*, 1127–1135.
(28) Jin, H.; Chen, W. Q.; Tang, X. W.; Chiang, L. Y.; Yang, C. Y.; Schloss, J. V.; Wu, J. Y. *J Neurosci. Res.* **2000**, *62*, 600–607.
(29) Dennler, G.; Markus, C. S.; Christoph, J. B. *Adv. Mater.* **2009**, *21*, 1–16.
(30) Ashcroft, J. M.; Tsyboulaski, D. A.; Hartman, K. B.; Zakharian, T. Y.; Marks, J. W.; Weisman, R. B.; Rosenblum, M. G.; Wilson, L. J. *Chem. Commun.* **2006**, 3004–3006.
(31) Gelderman, M. P.; Simakova, O.; Clogston, J. D.; Patri, A. K.; Siddiqui, S. F.; Vostal, A. C.; Simak, J. *Int. J. Nanomed.* **2008**, *3*, 59–68.
(32) Dugan, L. L.; Lovett, E. G.; Quick, K. L.; Latharius, J.; Lin, T. T.; O'Malley, K. L. *Parkinsonism Relat. Disord.* **2001**, *7*, 243–246.
(33) Ratnikova, T. A.; Bebber, M. J.; Huang, G.; Larcom, L. L.; Ke, P. C. *Nanotechnology* **2011**, *22*, 405101–1–7.
(34) Oberdorster, E. *Environ. Health Perspect.* **2004**, *112*, 1058–1062.

(35) Gharbi, N.; Pressac, M.; Hadchouel, M.; Szwarc, H.; Wilson, S. R.; Moussa, F. *Nano Lett.* **2005**, *5*, 2578−2585.
(36) Sayes, C. M.; Fortner, J. D.; Guo, W.; Lyon, D.; Boyd, A. M.; Ausman, K. D.; Tao, Y. J.; Sitharaman, B.; Wilson, L. J.; Hughes, J. B.; et al. *Nano Lett.* **2004**, *4*, 1881−1887.
(37) Qiao, R.; Roberts, A. P.; Mount, A. S.; Klaine, S. J.; Ke, P. C. *Nano Lett.* **2007**, *7*, 614−619.
(38) Salonen, E.; Lin, S.; Reid, M. L.; Allegood, M. S.; Wang, X.; Rao, A. M.; Vattulainen, I.; Ke, P. C. *Small* **2008**, *4*, 1986−1992.
(39) Wong-ekkabut, J.; Baoukina, S.; Triampo, W.; Tang, I. M.; Tieleman, D. P.; Monticelli, L. *Nat. Nanotechnol.* **2008**, *3*, 363−368.
(40) Meng, X; Li, B.; Chen, Z.; Yaw, L.; Zhao, D.; Yang, X.; He, M.; Yu, Q. *J. Enzyme Inhib. Med. Chem.* **2007**, *22*, 293−296.
(41) Shang, J.; Ratnikova, T. A.; Anttalainen, S.; Salonen, E.; Ke, P. C.; Knap, H. *Nanotechnology* **2009**, *20*, 415101−1−8.
(42) Ratnikova, T. A.; Govindan, P. N.; Salonen, E.; Ke, P. C. *ACS Nano* **2011**, *5*, 6306−6314.
(43) Chen, R.; Ratnikova, T. A.; Stone, M. B.; Lin, S.; Lard, M.; Huang, G.; Hudson, J. S.; Ke, P. C. *Small* **2010**, *6*, 612−617.
(44) Brant, J. A.; Labille, J.; Robichaud, C. O.; Wiesner, M. *J. Colloid Interface Sci.* **2007**, *314*, 281−288.
(45) Pinteala, M.; Dascalu, A.; Ungurenasu, C. *Int. J. Nanomed.* **2009**, *4*, 193−199.
(46) Hoffmann, M.; Hotze, E. M.; Wiesner, M. R. *Reactive Oxygen Species Generation on Nanoparticulate Material. In Environmental Nanotechnology: Applications and Impacts of Nanomaterials*; Wiesner, M. R., Bottero, J. Y., Eds.; The McGraw Hill Companies: 2007; pp 185−200.
(47) Lakowicz, J. R. Quenching of Fluorescence. In *Principles of Fluorescence Spectroscopy*; Springer: 2006.
(48) Lehrer, S. S. *Biochemistry* **1971**, *10*, 3254−3263.